DWBA-calculations of elastic scattering, fusion and breakup cross sections for reactions involving weakly bound stable projectiles around the barrier energy

A. Gómez Camacho, E.F. Aguilera, and E.M. Quiroz
Departamento del Acelerador, Instituto Nacional de Investigaciones Nucleares,
Apartado Postal 18-1027, 11801, México, D.F.
e-mail: agc@nuclear.inin.mx

Recibido el 13 de febrero de 2006; aceptado el 8 de agosto de 2006

A simultaneous Distorted Wave Born Approximation calculation of elastic scattering, fusion and breakup cross sections for energies above and below the Coulomb barrier energy is presented for reactions involving weakly bound projectiles on heavy targets. In the approach, a Woods-Saxon optical potential U is used where its imaginary part W is split into a volume part W_F which is only responsible for fusion absorption and a surface part W_{DR} which accounts for direct reactions. The fusion and direct reaction cross sections are calculated in terms of W_F and W_{DR} respectively. The optical potential parameters are determined from a simultaneous χ^2-analysis of recent experimental data of elastic scattering and fusion cross sections. From this, energy dependent forms for $W_F(E)$ and $W_{DR}(E)$ can be determined and by the dispersion relation the corresponding real polarization potentials $V_F(E)$ and $V_{DR}(E)$ are also found. The appearance or absence of the threshold anomaly can therefore be extracted from these energy dependent forms. By turning on and off the potentials responsible for breakup reactions (V_{DR} and W_{DR}) the effect of breakup on fusion can be studied. So, regions of suppresion and of enhancement around the barrier energy can be determined for the nuclear systems under study.

Keywords: Nuclear reactions; exotic nuclei; threshold anomaly.

Dentro de la aproximación de ondas distorsionadas de Born, se hace un estudio simultáneo de reacciones de dispersión elástica, fusión y de rompimiento del projectil conocido como breakup para reacciones nucleares que involucran projectiles debilmente ligados con blancos pesados. Se utilizan potenciales de Woods-Saxon U en los que la parte imaginaria W que es responsable de todos los procesos de absorción es dividida en dos partes, una W_F responsable sólo de los procesos de fusión y otra W_{DR} de los demás procesos, es decir de las reacciones directas. Los parámetros de tales potenciales serán determinados através de un ajuste simultáneo de los datos experimentales de fusión y de dispersión elástica. Se formulan entonces formas dependientes de la energía para W_F y W_{DR} através de las cuales de pueden determinar las partes reales de los potenciales de polarización V_F y V_{DR} usando la relación de dispersión. Del comportamiento con la energía de estás cuatro formas puede entonces determinarse la presencia o ausencia de la anomalía de umbral para el potencial de fusión y de reacciones directas respectivamente y en consecuencia del potencial total de absorción W. Finalmente considerando o anulando los potenciales V_{DR} y W_{DR} se realiza un estudio de la influencia que el proceso de rompimiento del projectil (breakup) tiene sobre el de fusión.

Descriptores: Reacciones nucleares; núcleos exóticos; anomalía de umbral.

PACS: 24.10.-i; 25.70.Jj; 23.23.+x; 56.65.Dy

1. Introduction

Nuclear reactions between neutron rich stable and unstable projectiles with heavy and medium targets have been the object of recent experimental and theoretical works. Neutron rich nuclei have the property of exhibiting a halo structure that may extend to large distances. These nuclei also show low lying dipole modes and small neutron threshold energies for breakup [1]. In particular, weakly bound stable nuclei with small neutron separation energies are of great interest as well due to the high breakup probability. The effect that the breakup mechanism has on other reaction processes particularly on fusion has been the object of several recent experimental and theoretical works. In fact, some theoretical papers suggest contradictory ideas about the effect that breakup of weakly bound projectiles has on fusion with medium and heavy targets. The controversy arises from whether the strong coupling to the breakup channel enhances or hinders the fusion process above and particularly below the Coulomb barrier energy region [2–7]. Only until recently, it has been possible to use radioactive beams of unstable nuclei on medium and heavy targets. Since the intensities of such beams are very low, measurements of fusion below the barrier energy have become difficult and time consuming. Then, in order to understand the high breakup probability of nuclear beams and the effect that breakup has on fusion, it is convenient to use high intensity beams of weakly bound stable or long half-life unstable projectiles. For instance, beams of this kind are stable nuclei such as ^9Be, ^6Li and ^7Li that have low neutron threshold energies from 1.48 MeV to 2.45 MeV or unstable long half-life nuclei such as ^6He with small $2n$ separation energy (0.98 MeV). Without doubt, the understanding of fusion, breakup and neutron transfer mechanisms of these type of incident beams is a necessary step in order to undertake similar studies on unstable radioactive beams such as ^{11}Li and ^{11}Be.

Stable nuclei like ^9Be, ^6Li, ^7Li have a relatively small neutron separation energy and in particular ^9Be has the property that when the valence neutron is knocked out, the remaining nucleus ^8Be becomes unstable and decays into two α particles with $T_{1/2} = 0.07$ fs. Even more, ^9Be

is strongly deformed since its ^8Be core has a well known α-α structure. The breakup mechanism of ^9Be can proceed through the channels $^9Be \Rightarrow n +^8 Be$ with a threshold energy E_{th} =1.665 MeV or through $^9Be \Rightarrow \alpha +^5 He$ with $E_{th} = 2.467$ MeV. Now, since both ^8Be and ^5He are unbound these decay channels end up in two α particles plus one neutron. In a nuclear reaction of ^9Be with heavy targets such as ^{209}Bi or ^{208}Pb [8–13] several processes can occur after the breakup of ^9Be;

a) Elastic breakup (EBU) when none of the fragments are captured by the target.

b) Incomplete fusion (ICF) when one of the α particles fuses to the target.

c) Complete fusion (CF) when the whole projectile ^9Be fuses to the target or when all the fragments after breakup fuse to the target.

d) Neutron transfer (NT) when the neutron produced after breakup is transferred to the outer shells of the target.

Possibly, some of the most important aspects to be questioned about these processes are related to the effect that the significant breakup yield for this nucleus has on fusion. For example;

1) Is the fusion enhanced or suppressed at different energy regimes? or

2) Is this enhancement or suppression related to the complete fusion or to the total fusion?,

3) How is that breakup of the projectile influence the appearance or absence of the threshold anomaly?

Several recent papers have tried to address these questions for reactions of ^9Be, ^6Li, ^7Li or ^6He with different targets. Dasgupta *et al*., [11] arrive to the conclusion that for the system $^9Be +^{208} Pb$ the breakup of ^9Be has a strong influence on suppressing the *complete fusion* yield above the barrier energy. In fact, their calculations show that the CF is only about 68% of the expected fusion as predicted by coupled-channel calculations. For this same system, R.J. Woolliscroft *et al*., [12, 13] have made complete measurements of elastic scattering angular distributions, α-breakup and one-neutron transfer yields. Their data show that for energies well below the fusion barrier energy there are substantial breakup and 1n-transfer yields. However, their optical model analysis show that despite the high breakup and 1n-transfer cross section values, the usual threshold anomaly still appears. This means that, in spite of the high values of the direct reaction measurements associated to elastic breakup and 1n-transfer reactions, the energy dependence of the absorption part of the optical potential still sharply decreases around the fusion barrier energy for decreasing bombarding energies as usually occurs for systems that show the threshold anomaly. On the other hand, the studies of N. Keeley *et al.*, [14, 15] for beams of weakly bound nuclei such as ^6Li ($^6Li \Rightarrow \alpha + d$, with threshold energy $E_{th} = 1.48$ MeV) and ^7Li ($^7Li \Rightarrow \alpha + t$, with $E_{th} = 2.45$ MeV) show that for the reaction $^6Li +^{208} Pb$ the usual threshold anomaly does not appear, not being the case for $^7Li +^{208} Pb$. Accordingly, the system $^6Li +^{208} Pb$ shows a high α-breakup yield below the barrier energy. Since ^9Be has a break-up threshold energy ($^9Be \Rightarrow^8 Be + n \Rightarrow \alpha + \alpha + n$, $E_{th} = 1.67$ MeV) closer to that for ^6Li, N. Keeley *et al.*, [14, 15] assume that the threshold anomaly should be absent for reactions involving ^9Be. For the similar nuclear system $^9Be +^{209} Bi$, Signorini *et al.*, [5, 9, 10] do not arrive to a definitive conclusion due to the small number of data precisely below the barrier energy region. Recently, the Brazilian group [6, 16–19] have intensely studied reactions of weakly bound beams such as ^6Li, ^7Li and ^9Be with medium mass targets as ^{27}Al and ^{64}Zn. In particular for the system $^9Be +^{64} Zn$, they have determined that the prior breakup of ^9Be into $^8Be + n$ and then to $\alpha + \alpha + n$ does not affect the total fusion (sum of the complete plus incomplete fusion cross sections) in any energy regime. However, the complete fusion becomes suppressed basically below the barrier energy due to the part of total fusion that corresponds to incomplete fusion. Above the barrier energy, the ICF results negligible leaving the TF almost the same as the CF. In agreement with the expectations of Refs. 14 and 15, the threshold anomaly is not found for $^9Be +^{64} Zn$ around the barrier energy.

In this work, we will study some reactions involving weakly bound projectiles such as ^9Be, ^6Li and ^6He with targets ^{208}Pb and ^{209}Bi within the Distorted Wave Born Approximation (DWBA) for direct reactions. Within this approach, we intend to elucidate the various and sometimes diverging conclusions found for these systems as cited above. That is, within the well known direct reaction approach as the DWBA, a simultaneous calculation of elastic scattering, fusion, and breakup cross sections will be performed. We will inquire into the effect that the breakup process has on the fusion one and on the so-called threshold anomaly for the systems $^6Li +^{208} Pb$, $^9Be +^{208} Pb$ and $^6He +^{209} Bi$. In the calculations, a Woods-Saxon optical potential $U_a = V_a + W_a$ for the entrance channel a is used. The imaginary part W_a is split into volume and surface parts, that is $W_a = W_{a,F} + W_{a,DR}$. Also, it will be assumed that the volume part $W_{a,F}$ of W_a is solely responsible for the fusion absorption process while the surface part $W_{a,DR}$ for all other absorption processes. The determined relative motion distorted waves $\chi_a^{(+)}$ obtained with the Woods-Saxon potential U_a will be used throughout the calculations, in this sense all of the calculated values will be consistent with elastic scattering. We propose that by means of the decomposition of W_a, the breakup effect of the projectile on fusion will be more clearly isolated in terms of the behavior of $W_{a,DR}$. Similarly, it is expected that the conjugated energy dependence of the fusion part $W_{a,F}$ and direct reaction part $W_{a,DR}$ will tell us about how strong is the breakup effect on fusion. That is, if there is fusion suppression or enhancement around the barrier energy. Also, it

is expected that the energy dependence of $W_{a,F}$ and $W_{a,DR}$ and the corresponding real parts $V_{a,F}$ and $V_{a,DR}$ will tell us if the the usual threshold anomaly is present.

The paper is organized as follows, in Sec. 2 a brief description of the model is presented. Section 3 is dedicated to the calculations, in which a simultaneous χ^2-analysis of recent elastic scattering and fusion cross sections will be done. The extracted Woods-Saxon parameters should simultaneously fit the fusion and elastic scattering cross section data. The total reaction cross section can be determined from the elastic scattering one since $\sigma_R = \sigma_{Ruth} - \sigma_{el}$ where σ_{Ruth} corresponds to the pure Rutherford Coulomb calculation and σ_{el} to our actual calculation. The difference $\sigma_{DR} = \sigma_R - \sigma_F$ corresponds to the direct reaction cross section which for the nuclear systems under consideration and for energies below the barrier is very close to the breakup plus 1n-transfer cross section. Also in this section, a discussion of the threshold anomaly is presented. As is well known the threshold anomaly refers to the closing of reaction channels as the bombarding energy decreases around the Coulomb barrier energy. This is related to a sharp decrease in the strength of the absorption potential W_a around the barrier. Through the dispersion relation, it is found that the strength of the corresponding real nuclear polarization part of the optical potential shows a sharp increase just around the barrier energy. Within our approach, by splitting W_a into a fusion part $W_{F,a}$ and a direct reaction part $W_{DR,a}$, we can separate the influence of each part in the determination of threshold anomaly. In the last part of the calculations, we discuss the effect of breakup on fusion yields by isolating the separate influence of each V_{DR} or W_{DR} or both together on the calculated fusion cross section. So, regions of energy where there is fusion suppression or enhancement can be distinguished. Finally, Sec. 4 is dedicated to a summary of this work.

2. Basic formalism

The Hamiltonian H for the nuclear system is of the form,

$$H_a = T_a + \mathcal{V}_a, \tag{1}$$

where the potential $\mathcal{V}_a$ is defined by,

$$\mathcal{V}_a(r,E) = V_{Coul}(r) - V_{a,0}(r) - U_a(r,E), \tag{2}$$

$V_{Coul}(r)$ is the Coulomb potential between the reacting ions, $V_{a,0}(r)$ is the energy independent Hartree-Fock potential and $U_a(r,E)$ is the nuclear polarization potential given by [20–22],

$$U_a(r,E) = V_a(r,E) + iW_a(r,E). \tag{3}$$

For the moment and to facilitate the notation, we will drop the index a which indicates the incident elastic channel. The imaginary part W will be assumed to be composed of two parts, a fusion part and the direct reaction part, *i.e.*,

$$W(r,E) = W_F(r,E) + W_{DR}(r,E), \tag{4}$$

where W_F will be responsible for fusion reactions and W_{DR} for all other absorption processes, that is direct reactions. The real polarization potential $V(r,E)$ can be derived from the corresponding imaginary polarization potential $W(r,E)$ by the dispersion relation,

$$V(r,E) = \frac{(E-E_b)}{\pi}\mathcal{P}\int_0^\infty \frac{W(r,E')}{(E'-E_b)(E'-E)}dE', \tag{5}$$

here E_b is a reference energy as defined in Ref. 23. Therefore, for each part of the imaginary potential $W(r,E)$ of Eq. (4), there corresponds a real part, that is $V_F(r,E)$ for $W_F(r,E)$ and $V_{DR}(r,E)$ for $W_{DR}(r,E)$, each given by a relation like Eq. (5). Thus, by using Eq. (4), we would have that the total real nuclear polarization potential satisfies,

$$V(r,E) = V_F(r,E) + V_{DR}(r,E). \tag{6}$$

The energy independent nuclear potential $V_0(r)$ and the fusion absorption potential $W_F(r,E)$ are assumed to have the geometrical forms,

$$V_0(r) = V_0 f(r) \tag{7}$$

and,

$$W_F(r,E) = W_F(E) f(r) \tag{8}$$

where,

$$f(r) = \frac{1}{1+\exp(x_i)},\ x_i = \frac{r-R_i}{a_i},\ i = 0, F \tag{9}$$

here a_i refers to the diffuseness parameter and $R_i = r_i(A_1^{1/3} + A_2^{1/3})$ the radial parameter. The surface imaginary potential $W_{DR}(r,E)$ is defined by,

$$W_{DR}(r,E) = 4a_{DR}W_{DR}(E)\frac{df(r)}{dR_{DR}}, \tag{10}$$

where a_{DR} stands for the direct reaction diffuseness and R_{DR} for the corresponding radial parameter. The parameters V_0, $W_F(E)$ and $W_{DR}(E)$ will be extracted from a simultaneous χ^2-analysis of the elastic and fusion experimental data as it will be shown in the next section It should be pointed out that the breakup cross section may include contributions from Coulomb and nuclear interactions, this implies that the direct reaction potential includes both effects. Also, the Hartree-Fock potential $V_0(r)$ in Eq. (2) may have an energy dependence due to the non-locality effect coming from the knockon-exchange contribution, we will not consider such effects since they are negligible [24]. The angle-integrated total reaction cross section is calculated by using the full absorption potential W, *i.e.*,

$$\sigma_R(E) = \frac{2}{\hbar v}\left\langle \chi_a^{(+)} \left| W(E) \right| \chi_a^{(+)} \right\rangle \tag{11}$$

where we have rewritten the sub-index a to emphasize the elastic channel. $\chi_\alpha^{(+)}$ is the distorted wave function which is solution of $H_a\chi_a^{(+)} = E_a\chi_a^{(+)}$, H_a being the Hamiltonian of

Eq. (1), v is the relative velocity between the colliding ions. The fusion and direct reaction cross sections are similarly obtained by,

$$\sigma_i(E) = \frac{2}{\hbar v} \left\langle \chi_a^{(+)} \left| W_i(E) \right| \chi_a^{(+)} \right\rangle, \; i = F, DR. \qquad (12)$$

3. Simultaneous χ^2-analysis of elastic scattering, fusion, and direct reaction cross sections

Recently, there has been an extensive experimental work on reactions involving weakly bound projectiles. For the nuclear systems studied in the present work, we will consider the data of Refs. 25 and 26 for the $^6He + ^{209}Bi$ system, Refs. 14 and 15 for $^6Li + ^{208}Pb$, and Refs. 11 and 12 for the $^9Be + ^{208}Pb$ system. Now, the direct reaction cross section can be further generated by,

$$\sigma_{DR} = \sigma_R - \sigma_F. \qquad (13)$$

Therefore, if there are sufficient data for the elastic scattering and the fusion cross section below and above the Coulomb barrier energy, the total reaction and the direct reaction cross sections can be determined in the same region of energies. It should be mentioned that the way in which σ_{DR} has been generated in this work is about 10 to 30% larger than the measured breakup cross section for the system $^6Li + ^{208}Pb$ [27], the difference should be due to incomplete fusion. As for $^9Be + ^{208}Pb$, σ_{DR} is very close to the sum of the breakup and transfer cross sections [13] As a first step, and in order to explore into the behavior of the absorption potentials W_F and W_{DR} with the energy, we will determine the best optical potential parameters for the real Hartree-Fock potential and imaginary fusion and direct reaction parts of the optical potential by a simultaneous χ^2-fitting of elastic scattering and total fusion data. For the real nuclear Hartree-Fock potential, we fix the values $V_0 = 18.36$ MeV, $r_0 = 1.22$ fm and $a_0 = 0.57$ fm for the $^6Li + ^{208}Pb$ system and $V_0 = 29.53$ MeV, $r_0 = 1.25$ fm and $a_0 = 0.65$ fm for the $^9Be + ^{208}Pb$ while for $^6He + ^{209}Bi$ a deeper potential strength is nedeed that is, $V_0 = 100.4$ MeV, $r_0 = 1.1$ fm and $a_0 = 0.54$ fm. On the other hand, for $^6Li + ^{208}Pb$, we fix the radial and diffussenes parameters $r_F = 1.4$ fm and $a_F = 0.42$ fm of W_F and $r_D = 1.47$ fm and $a_D = 0.85$ fm of W_{DR} remaining $W_F(E)$ and $W_D(E)$ to be fitted. For $^9Be + ^{208}Pb$, we set $r_F = 1.4$ fm, $a_{DR} = 0.5$ fm, $r_D = 1.51$ fm while $W_F(E)$, $W_D(E)$ and a_F are calculated by the χ^2-analysis. Finally, regarding $^6He + ^{209}Bi$, we fix $r_F = 1.4$ fm, $a_F = 0.55$ fm, $W_D = 0.4$ MeV and $a_D = 1.25$ fm remaining $W_F(E)$ and r_D to be fixed. In Table I, all the calculated parameters are listed as function of the collision energy.

TABLE I. Optical potential parameters. Energies and potential depths in MeV. Radial parameters in fm.

$^6Li + ^{208}Pb$			$^6He + ^{209}Bi$		
$E_{cm} - V_B$	W_F	W_{DR}	$E_{cm} - V_B$	W_F	r_{DR}
-8.95	0.0023	0.015	-8.62	0.0227	1.729
-6.13	0.016	0.105	-5.98	0.0237	1.648
-2.37	0.0324	0.395	-4.5	0.0242	1.622
-1.43	0.069	0.462	-3.02	0.0544	1.592
0.56	0.152	0.507	-1.644	0.0845	1.506
2.45	0.219	0.56	1.11	0.0855	1.5
4.44	0.22	0.59	3.22	0.0864	1.483
8.32	0.221	0.67	5.87	0.0874	1.47
			8.94	0.0885	1.43
$^9Be + ^{208}Pb$					
E_{lab}	E_{cm}	$E_{cm} - V_B$	W_F	W_{DR}	a_F
38	36.42	-1.88	0.0056	0.2287	0.365
40	38.34	0.0	0.0138	0.3497	0.299
42	40.26	1.96	0.0399	0.4237	0.297
44	42.17	3.87	0.0319	0.4073	0.289
46	44.1	5.8	0.009	0.4477	0.2252
48	46.0	7.71	0.1297	0.335	0.2598
50	47.92	9.62	0.0998	0.4864	0.3821
60	57.51	19.21	0.2047	0.5552	0.0996
68	65.2	26.88	0.1847	0.5649	0.1865
70	67.1	28.8	0.2897	0.4627	1.15

Before doing final calculations of elastic, total reaction, fusion and direct reaction cross sections, we assume linear parametrizations for the fitted optical potential strength parameters for each system, so for $^6Li +^{208} Pb$ we have (in MeV),

$$W_F(E_{cm})=\begin{cases} 0 & E_{cm} \leq E_{0,F} = 26.8 \\ 0.4(E_{cm} - 26.8) & 26.8 < E_{cm} \leq 34 \\ 2.9 & 34 < E_{cm} \end{cases} \tag{14}$$

and,

$$W_{DR}(E_{cm})=\begin{cases} 0 & E_{cm} < E_{0,DR} = 22 \\ 0.08(E_{cm} - 22) & 22 < E_{cm} < 28 \\ 0.023(E_{cm} - 28) + 0.5 & 28 < E_{cm} < 37.9 \\ 0.73 & 37.9 < E_{cm} \end{cases} , \tag{15}$$

where $E_{0,F}$ and $E_{0,DR}$ correspond to the fusion and direct reaction threshold energies. Similarly for $^9Be +^{208} Pb$ we have,

$$W_F(E_{cm})=\begin{cases} 0 & E_{cm} \leq E_{0F} = 36.92 \\ 0.0082(E_{cm} - 36.92) & 36.92 < E_{cm} \leq 62.1 \\ 0.207 & 62.1 < E_{cm} \end{cases} \tag{16}$$

and,

$$W_{DR}(E_{cm})=\begin{cases} 0 & E_{cm} \leq E_{0F} = 16.94 \\ 0.0131(E_{cm} - 16.94) & 16.94 < E_{cm} \leq 52.28 \\ 0.4629 & 52.28 < E_{cm} \end{cases} . \tag{17}$$

Finally, for $^6He +^{209} Bi$ the corresponding equations are,

$$W_F(E_{cm})=\begin{cases} 0 & E_{cm} \leq E_{0F} = 15.4 \\ 1.25(E_{cm} - 15.4) & 15.4 < E_{cm} \leq 18.5 \\ 4.0 & 18.5 < E_{cm} \end{cases} \tag{18}$$

and,

$$r_D(E_{cm})=\begin{cases} 1.73 & E_{cm} \leq 14.0 \\ 1.73 - 0.03(E_{cm} - 14.0) & 14.0 < E_{cm} \leq 21.4 \\ 1.51 & 21.4 < E_{cm} \end{cases} \tag{19}$$

It should be remembered that for any given energy $W_T = W_F + W_{DR}$. Now, by using the parametrizations for the potential depths W_F and W_{DR} as function of the energy just given, the corresponding real polarization potentials V_F, V_{DR} and $V_T = V_F + V_{DR}$ can be found through the use of the dispersion relation, Eq. (5). The integration of the linear forms Eqs. (15)-(19) has already been given in Ref. 23, the results are of the form,

$$\begin{aligned} \pi V(E) = {} & W_0 \left[\epsilon_a \ln|\epsilon_a| - \epsilon_b \ln|\epsilon_b|\right] \\ & + (W_1 - W_0)[\epsilon'_b \ln|\epsilon'_b| - \epsilon'_c \ln|\epsilon'_c|] \\ & - W_1[\epsilon''_c \ln|\epsilon''_c| - \epsilon''_m \ln|\epsilon''_m|] \\ & + W_1[\eta \ln \eta - (\eta+1)\ln(\eta+1)], \end{aligned} \tag{20}$$

where, ϵ_a and ϵ_b are defined by,

$$\epsilon_a = \frac{E - E_a}{E_b - E_a} \quad \text{and} \quad \epsilon_b = \frac{E - E_b}{E_b - E_a} \tag{21}$$

with E_a and E_b ($E_a < E_b < \infty$) being the limiting energies of the first linear segment. Similar equations for $\epsilon'_b, \epsilon'_c, \epsilon''_c$ etc. are valid for the second, third etc. linear segments. For each reacting nuclear system final calculations of cross sections will be done with the use of the energy dependent forms just

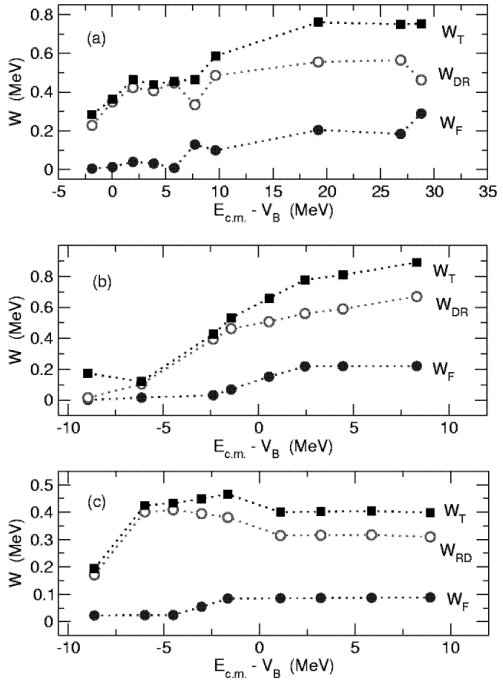

FIGURE 1. Imaginary absorption potentials, W_F, W_{DR} and W_T as functions of the energy for the systems a) $^9Be +^{208} Pb$, b) $^6Li +^{208} Pb$ and c) $^6He +^{209} Bi$.

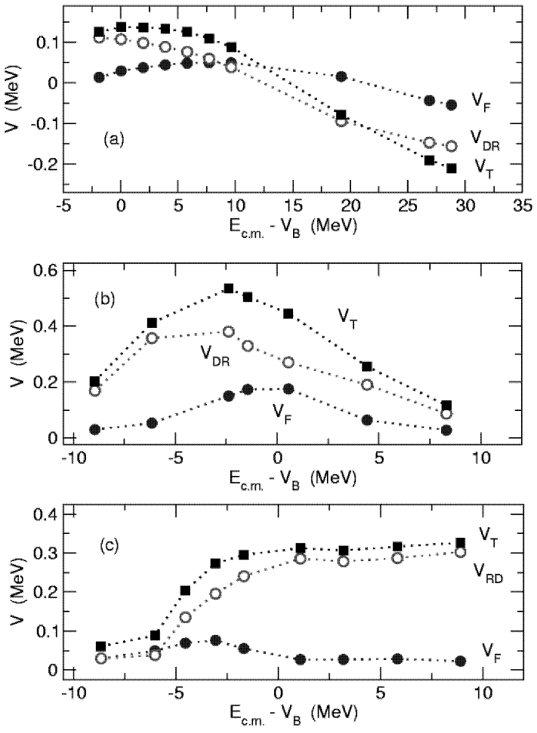

FIGURE 2. Real polarization potentials, V_F, V_{DR} and V_T as functions of the energy for the systems a) $^9Be+^{208}Pb$, b) $^6Li+^{208}Pb$ and c) $^6He+^{209}Bi$.

given for the fusion and direct reaction absorption potentials and the corresponding real parts calculated in Eq.(21). The imaginary potentials $W_F(E)$, $W_{DR}(E)$ and its sum W_T at the strong absorption radius are shown in Figs. 1a-1c while the corresponding V_F, V_{DR} and V_T are presented in Figs. 2a-2c. From these figures it can be seen that the $^9Be+^{208}Pb$ system shows the threshold anomaly around the barrier energy ($V_{B,cm} = 38.3$ MeV). This is not the case for the systems $^6Li+^{208}Pb$ and $^6He+^{209}Bi$ since around the corresponding barrier energies ($V_{B,cm}$=29.6.3 and 20.3 MeV), W_T does not show a sharp decrease and consecuently V_T does not show the usual bell shape centered at the barrier ($E_{cm} = V_B$). In Figs. 3a,3b and 3c the elastic scattering calculation is presented for the systems $^9Be+^{208}Pb$ and $^6He+^{209}Bi$. Fig. 4a shows the results for the breakup and fusion cross sections for $^6He+^{209}Bi$, where it has been assumed that all of the direct reaction cross section corresponds solely to breakup for energies around and below the barrier energy. Fig. 4b shows the corresponding calculations for $^6Li+^{208}Pb$ in comparison with the data of [14,28]. As seen in these calculations, for energies around below the barrier energy, the direct reaction processes account for most of the total absorption. The small breakup threshold energy for the weakly bound projectiles treated in the present study is the main factor for the high breakup and neutron transfer yields that persist being important even for energies well below the barrier energy.

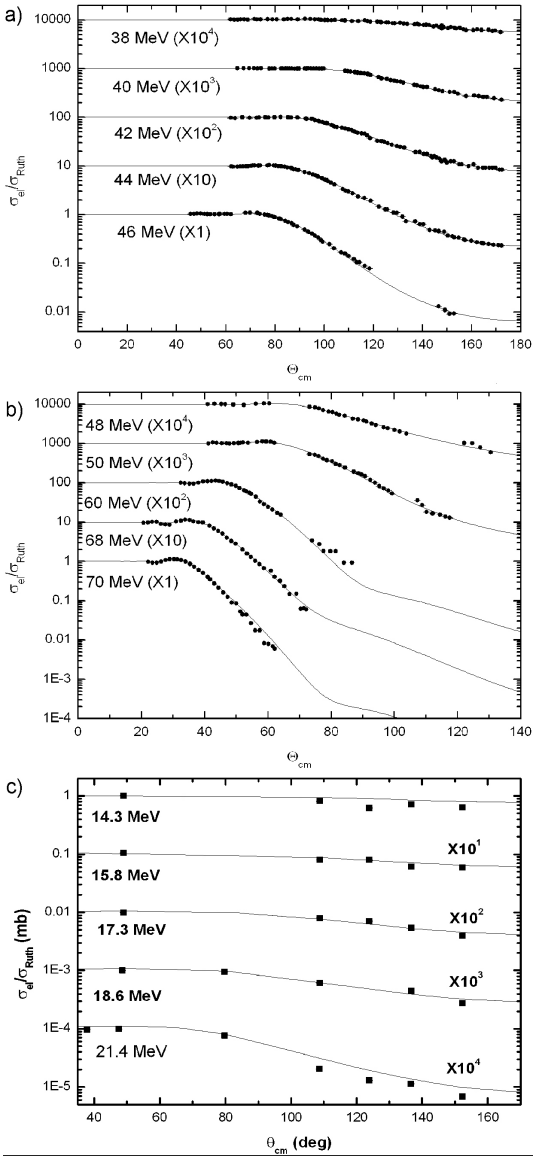

FIGURE 3. Elastic scattering cross section for a), b) $^9Be+^{208}Pb$ and c) $^6He+^{209}Bi$.

We pass now to consider the effect that breakup reactions have on fusion, this can be done by turning on and off the part of the potential that is responsible for direct reactions, that is V_{DR} and W_{DR}. We have to remember that breakup reactions are the most important contributors to direct reactions for the weakly bound projectiles involved in the present study. There are two physical effects by which V_{DR} and W_{DR} affect fusion reactions, an attractive V_{DR} tends to lower the Coulomb barrier and therefore enhances fusion, on the other hand a loss of flux into direct reactions represented by W_{DR} lowers or suppresses fusion reactions. So, by considering each V_{DR} and W_{DR} and then both together will tell us the independent effect on fusion. Therefore, we define the ratio,

$$R_i = \sigma_F(i)/\sigma_F(V_{DR} = W_{DR} = 0);$$
$$i = V_{DR}, W_{DR}, V_{DR}W_{DR}. \quad (22)$$

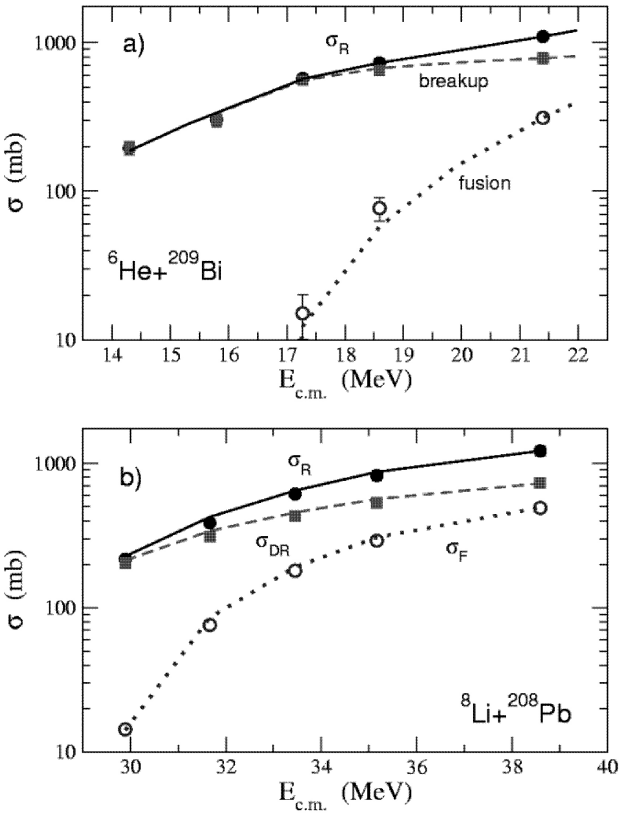

FIGURE 4. a) Total reaction, breakup and fusion cross sections for $^6He + ^{209}\ Bi$. b) Total reaction, direct reaction and fusion cross sections for $^6Li + ^{208}\ Pb$.

It should be remarked that $\sigma_F(V_{DR}W_{DR})$ corresponds to our final calculation that we have shown above. Fig. 5 shows the results for the three nuclear systems under study. In the range of energies considered, as expected, the real attractive potential V_{DR} lowers the fusion barrier and for that reason $R_{V_{DR}} > 1$ which means fusion enhancement for all energies. On the other hand, W_{DR} is connected to the loss of flux mainly into the breakup channel and therefore $R_{W_{DR}} < 1$ which means fusion suppression in the whole range of energies. When both potentials V_{DR} and W_{DR} are applied we can separate regions of enhancement and suppression, so for $^6He + ^{209}\ Bi$ the ratio $R_{V_{DR}W_{DR}}$ is smaller than one for all energies considered above and below the barrier energy. For $^9Be + ^{208}\ Pb$ there is a net fusion enhancement for energies $E_{cm} < V_B + 4$ and suppression for energies above this range. Finally the $^6Li + ^{208}Pb$ system there is fusion suppression for energies $E_{cm} > V_B - 1$ and supression otherwise.

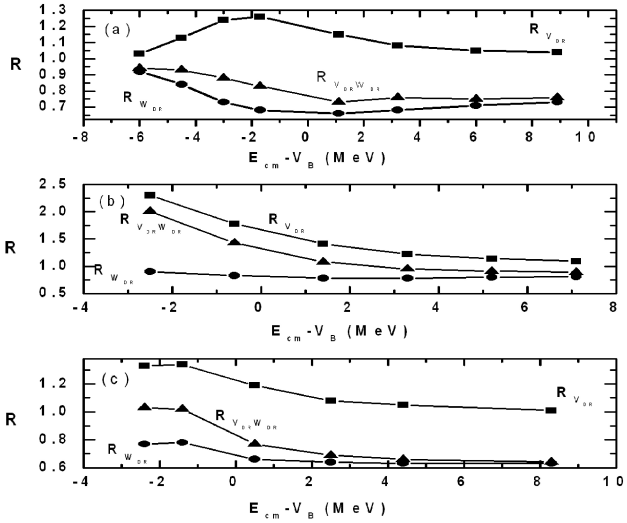

FIGURE 5. R_{VDR}, R_{WDR} and $R_{VDR,WDR}$ as defined in the text for the systems a) $^6He + ^{209}Bi$, b) $^9Be + ^{208}Pb$ and c) $^6Li + ^{208}Pb$.

4. Summary

In this work, we have presented a simultaneous DWBA calculation of elastic scattering. direct reaction (breakup) and fusion cross sections. In the model, the optical polarization potential has been split into a fusion part and a direct reaction part each responsible for the corresponding fusion and direct reactions. Energy dependent forms for each imaginary parts $W_F(E)$ and $W_{DR}(E)$ have been determined by a χ^2-analysis of elastic and fusion data. Then corresponding energy dependent forms for $V_F(E)$ and $V_{DR}(E)$ have been derived from the dispersion relation. These energy dependent forms show that the threshold anomaly shows up for the system $^9Be + ^{208}\ Pb$. However, this is not the case for the $^6He + ^{209}Bi$ and $^6Li + ^{208}Pb$ systems where $W_T(E)$ shows a slow decreasing and a stable behavior around the corresponding barrier energies V_B. On the other hand, in these two cases $V_T(E)$ does not show the usual bell shape around V_B as occurs when the threshold anomaly is present. The effect of breakup on fusion cross sections have been studied by turning on and off the potentials responsible for fusion enhancement V_{DR} and fusion suppresion W_{DR}. So, energy regions of fusion enhancement and suppression have been determined for the three nuclear systems of the present work.

Acknowledgments

This work has been supported in part by CONACYT under project 44251.

1. P.G. Hansen *et al., Annu. Rev: Nucl. Part. Sci.* **45** (1995) 591.
2. J.J. Kolata *et al.*, *Phys. Rev. Lett.* **81** (1998) 4580.
3. E.F. Aguilera *et al.*, *Phys. Rev. C* **63** (2001) 061603(R).
4. A. Yoshida *et al.*, *Phys. Lett. B* **389** (1996) 457.
5. C. Signorini, *et al., Eur. Phys. J.* **A.2** (1998) 227.
6. P.R.S. Gomes, J. Lubian, and R.M. Anjos, *Nucl. Phys. A* **734** 233 (2004).
7. M.S. Hussein, *Nucl. Phys. A* **531** (1991) 192.
8. D.P. Stahel *et al.*, *Phys. Rev. C* **16** (1977) 1456.
9. C. Signorini, *Eur. Phys. J. A* **13** (2002) 129.
10. C. Signorini *et al*., *Phys. Rev. C* **61** (2000) 061603(R).
11. M. Dasgupta *et al., Phys. Rev. Lett.***82** (1999) 1395.
12. R.J. Woolliscroft *et al., Phys. Rev. C* **68** (2003) 014611-1.
13. R.J. Woolliscroft *et al., Phys. Rev. C* **69** (2004) 044612.
14. N. Keeley *et al., Nucl. Phys. A* **571** (1994) 326.
15. N. Keeley and K. Rusek, *Phys. Lett. B* **427** (1998) 1.
16. P.R.S. Gomes *et al., Phys. Lett B* **601** (2004) 20.
17. S.B. Moraes *et al., Phys. Rev. C* **61** (2000) 064608.
18. I. Padron *et al., Phys. Rev. C* **66** (2002) 044608.
19. J. Lubian *et al., Phys. Rev. C* **64** (2001) 027601.
20. A. Gómez Camacho, E.M Quiroz, and T. Udagawa, *Nucl. Phys. A* **635** (1998) 346.
21. A. Gómez Camacho and T. Udagawa, *Rev. Mex. Fís.* **44** (1998) 85.
22. A. Gómez-Camacho, E.F. Aguilera, and A.M. Moro, *Nucl. Phys. A* **762** (2005) 216.
23. C. Mahaux, H. Ngô, and G.R. Satchler, *Nucl. Phys. A* **449** (1986) 354.
24. G.R. Satchler and W.G. Love, *Phys. Rep.* **55** (1979) 18.
25. E.F. Aguilera *et al., Phys. Rev. C* **84** (2000) 5058.
26. J.J. Kolata *et al., Phys. Rev. Lett.* **81** (1998) 4580.
27. C. Signorini *et al., Phys. Rev. C* **67** (2003) 044607.
28. Y.W. Wu *et al.*, *Phys. Rev. C* **68** (2003) 044605.